Allometric Models to Estimate Carbon Content in Arecaceae Based on Seven Species of Neotropical Palms

Milena Cambronero
School for Field Studies
Gerardo Avalos (faetornis@yahoo.com)
University of Costa Rica School of Biology: Universidad de Costa Rica Escuela de Biologia
https://orcid.org/0000-0003-2663-4565
Carolina Alvarez-Vergnani
University of Costa Rica School of Biology: Universidad de Costa Rica Escuela de Biologia

Research Article

Keywords: carbon stocks, carbon sequestration, allometric models

Posted Date: September 13th, 2021

DOI: https://doi.org/10.21203/rs.3.rs-838582/v1

Allometric models to estimate carbon content in Arecaceae based on seven species of neotropical palms

Milena Cambronero[2] (milemd4@yahoo.com)

Gerardo Avalos[1,2] (gerardo.avalos@ucr.ac.cr)

Carolina Alvarez-Vergnani[1] (caroav@gmail.com)

[1]Escuela de Biología, Universidad de Costa Rica, 11501-2060 San Pedro, San José, Costa Rica

[2]The School for Field Studies, Center for Sustainable Development Studies, 100 Cummings Center, Suite 534G, Beverly, MA 01915, USA.

Correspondence: Gerardo Avalos, gerardo.avalos@ucr.ac.cr, (506) 25115955

Author Contributions: GA conceived and designed the experiments. MC and CAV conducted the fieldwork with assistance from GA. GA, MC, and CAV analyzed the data and wrote the manuscript.

Abstract

We present allometric models to estimate total carbon content and above ground carbon (AGC) for the family Arecaceae, and for 7 abundant neotropical palm species (the canopy species *Socratea exorrhiza* and *Iriartea deltoidea*, the sub-canopy palm *Euterpe precatoria*, and the understory species *Asterogyne martiana*, *Prestoea decurrens*, *Geonoma interrupta* and *Chamaedorea tepejilote*). The study was done in the tropical rainforests of the Caribbean slope of Costa Rica. We harvested 87 individuals of a wide range of sizes, and divided them into roots, stems, and leaves, weight their fresh and dry biomass, calculated the carbon content, tissue density, leaf area, and shoot:root ratios (based on biomass and carbon content). The general palm model estimating total carbon content accounted for 92% of the variation and had diameter at breast height, stem height, and dry mass fraction as predictor variables. We generated a similar model to estimate AGC, which included the same variables and explained 91% of the variation. We compared our AGC model with two models used to estimate palm carbon content: Goldman et al. (2013)´s and Chave et al. (2014)´s models and found a range of R^2 values of 0.87 to 0.91. Understory palm allometry was centered around biomass allocation, whereas sub-canopy and canopy species were associated with traits related to palm size (mainly DBH, total height, and leaf area). The efficiency the allometric models depends on species identity, sample size, and size range.

Keywords: carbon stocks, carbon sequestration, allometric models

Introduction

Over the last century, land-use changes, logging, forest fires, and burning of fossil fuels have caused a dramatic increase in the atmospheric concentration of carbon dioxide

49 (CO_2), as well as of other greenhouse gases (GHG), leading to severe climate events (Clark
50 2007; Díaz et al. 2019). Accurate models to estimate carbon stocks are critical to
51 successfully implement carbon and climate change policies (Zhang et al. 2012; Chave et al.
52 2014). Numerous organizations, including the United Nations Framework Convention on
53 Climate Change (UNFCCC), have warned of the urgency of reducing GHG emissions and
54 mitigating the effects of climate change to maintain the viability of ecosystems and keep
55 suitable conditions for human life. To achieve these goals, it is essential to elucidate the
56 behavior of various carbon sinks and sources to understand the consequences of
57 anthropogenic effects on the climate (Clark 2007; Houghton 2007; Canadell and Raupach
58 2008; Goers et al. 2012; Steffen et al. 2018).
59 Tropical forests influence the atmospheric concentration of CO_2, are important
60 reservoirs of carbon, and play a significant role in mitigating the effects of climate change
61 (Houghton 2007; Goers et al. 2012) but are becoming net carbon sources as their capacity
62 to absorb and store carbon is diminished by logging, land-use changes, droughts, and forest
63 fires (Brando et al. 2019; Friedlingstein et al. 2020). It is still necessary to refine
64 methodologies to quantify carbon sequestration in tropical forests, as well as to increase the
65 available information across plant groups to understand how different species, ontogenetic
66 stages, and life forms contribute to the total accumulation of carbon in terrestrial
67 ecosystems (Dewar 1991; Dewar and Cannell 1992; Brown 1997; Achard et al. 2004).
68 Currently, there are numerous methods to estimate the carbon stocks in forested areas
69 (Zhang et al. 2012). Remote sensing techniques facilitate the monitoring of extensive areas
70 with low costs and large-scale resolution (Jucker et al. 2017; Rodríguez-Veiga et al. 2019)
71 but are limited by field validation using ground-based techniques. Allometric methods
72 represent a traditional, but time-consuming alternative. These methods are based on

mathematical models relating morphological measurements to biomass or stored carbon (Hairiah et al. 2001; Chave et al. 2005, 2014; Montero and Montagnini 2005; Zhang et al. 2012) and have some extensive databases (Chave et al. 2005; Curtis 2008; Lal 2008; Lorenz and Lal 2010, Kissling et al. 2019). Most allometric studies have focused on woody dicotyledonous trees, particularly the most common and commercially important species (Brown 1997; Hairiah et al. 2001; Chave et al. 2005; Zhang et al. 2012; Chave et al. 2014), and usually include only a handful of individuals of a limited size range per species. Life forms such as lianas, hemiepiphytes, ferns, and palms have been excluded from these inventories (Clark et al. 2001; Chave et al. 2005, 2014; Jucker et al. 2017). Few studies (Nascimento and Laurance 2002; Lima et al. 2012) have included a variety of life forms, like palms and lianas.

Palms (Arecaceae) are one of the most diverse and widely distributed groups of plants in tropical and subtropical areas, with around 2,600 species and 181 genera (Baker and Dransfield 2016). Many tropical ecosystems are dominated by palms (Mejia and Kahn 1990; Myers 2013), such as seasonally or permanently inundated wetlands, such as the "aguajales" in the Peruvian Amazon (dominated by *Mauritia flexuosa*, Sampaio et al. 2008), the "yolillales" in Costa Rica (dominated by *Raphia taedigera*, Serrano-Sandí et al. 2013; Yaap et al. 2015), and peatlands in tropical swamp forests in the Congo basin (some dominated by *R. laurentii* and *R. hookeri*), which are important reservoirs of soil carbon (Lähteenoja et al. 2009; Dargie et al. 2017). Due to their abundance in the Amazon lowlands, palms have been considered "hyperdominant" elements (ter Steege et al. 2013), with 6 out of the 10 most abundant species being palms. Although they have a limited contribution to carbon stocks in diverse tropical rainforests (Fauset et. 2015), palms can influence forest function (Boukili and Chazdon 2017), play a crucial role in food webs,

97 providing habitat and food to a multitude of animal species (Zona and Henderson 1989;
98 Howard et al. 2001; Onstein et al. 2017), and are invaluable to many human groups who
99 use them as raw materials for construction, food, drink, clothing, fuel, medicine, and fibers
100 (Jones 1995; Henderson 2002; Dransfield et al. 2008; Sylvester et al. 2012)

101 Despite their functional role, palms have been excluded from most inventories of
102 carbon accumulation in tropical forests (DeWalt and Chave 2004; Chave et al. 2005;
103 Lorenz and Lal 2010), as well as from comprehensive allometric analysis of diameter vs.
104 height relationships (Feldpausch et al. 2011). The few studies on carbon content in palms
105 are limited to the wetland species *M. flexuosa* and *M. aculeata* (Goodman et al. 2013), and
106 commercially important species, such as peach palm, *Bactris gasipaes* (Ares et al. 2002),
107 and oil palm, *Elaeis guineensis* (Thenkabail et al. 2004; Syahrinudin 2005; Leblanc et al.
108 2006; Ekadinata et al. 2010; Khasanah et al. 2012; Pulhin et al. 2014). As monocots, palms
109 have a different structure, allometry, and strategies of resource use relative to trees
110 (Tomlinson 2006, 2011). With a few exceptions, palms are monopodial and lack aerial
111 branching, have only one shoot meristem, and lack dormancy and secondary growth. In
112 palm species where stem diameter and stem height show a significant relationship, diameter
113 increases through sustained primary growth (i.e., through the division, lignification, and
114 expansion of parenchyma cells, which also differentiate into fibers, Tomlinson 2011). In
115 addition, leaf longevity and leaf construction costs are higher in palms than in
116 dicotyledonous trees (Renninger and Phillips 2016), which have smaller leaves than palms
117 and could drop leaflets rather than the entire frond to acclimate to new light conditions.
118 Palm responses to environmental gradients are fundamentally different from those of
119 woody plants. It is essential to understand their allometric relationships to develop accurate
120 and more specific models to estimate their contribution to carbon storage.

121 The objectives of this research are: a) to generate allometric models to estimate
122 carbon storage in seven species of neotropical palms from different forest strata, b) to
123 produce general models to estimate above-ground carbon and total carbon for palms based
124 on these species using traits commonly measured in forest inventories, and c) compare
125 these models with two of the most widely used models to estimate the contribution of
126 palms to carbon storage: the Goodman et. (2013)´s model, developed for a subset of 8
127 species of neotropical palms, and the pantropical model of Chave et al. (2014), developed
128 for dicotyledonous trees. These specific palm models may have similar limitations to the
129 models generated for dicotyledonous trees, are biased by the species composition, the
130 number and size of the harvested individuals, and the environmental conditions of the
131 collection sites. Despite these limitations, the generation of specific models for palms is
132 necessary as the lack of data for this group makes it difficult to estimate their contribution
133 to the carbon balance of tropical forests, especially in habitats where palms are very
134 abundant.
135 We expected that the diameter at breast height (DBH) and stem height would be the
136 best predictors of carbon storage, since it has been shown that both variables are related to
137 biomass accumulation (Goodman et al. 2013), are functionally related to carbon storage,
138 determine mechanical support (Avalos et al. 2019), and reflect palm size. We did not
139 expect wood density (or the density of the sclerotized tissue in palms) to be an important
140 predictor of carbon content, since palms do not develop wood, but rather have a sclerotized
141 tissue that is not evenly distributed along the stem, and which increases in density and
142 mechanical strength from the base and the periphery of the stem towards the crown (Rich
143 1986; Henderson 2002). Finally, we expected that the use of Chave et al. (2014)´s model,
144 developed for trees, would lead to an underestimation of carbon storage in palms, due to the

significant structural and allometric differences between dicotyledonous trees and palms, and the inclusion of tissue density in Chave et al. (2014)´s model.

Materials and methods

Study site

Palms were harvested in three tropical rain forest sites in the Caribbean lowlands of Costa Rica. The first two were La Selva Biological Station (10°26'N - 83°59'W, 30-150 masl, annual precipitation 4,162 mm) and Tirimbina Biological Reserve (10°24'N - 84°06W, 180-220 masl, annual precipitation 3,833 mm), both situated in Sarapiquí, Heredia. The third site was the lowland forest of the agroecological farm El Progreso (10°30'35'' N - 83°44'39'' W, 45 masl, annual precipitation of 4,000 to 5,000 mm), located in Pococí, Limón. The three sites present an average daily temperature of 25°C and have a weak climatic seasonality, with November, December and February being the rainiest months (McDade et al. 1994).

Study species

We selected seven palm species belonging to different forest strata (Table 1). The canopy species *Socratea exorrhiza* (S Nicaragua to Brazil, 0-750 masl) and *Iriartea deltoidea* (SE Nicaragua to Brazil, 0-800 masl) can reach 25 and 30 m of stem height, respectively, and are characteristic canopy components of mature forests (Grayum 2003). Both species have a cone of stilt roots, although roots in *I. deltoidea* are clustered at the base of the stem and grow up to 1.5 m above ground, and in *S. exorrhiza* roots are well-separated, covered by spines, and can grow up to 4 m above the ground (Henderson et al. 1995). The subcanopy

169 species *Euterpe precatoria* (Belize to Bolivia, 0-1150 masl) var *longevaginata* (Henderson
170 1995) is single-stemmed and can reach 26 m in height, developing a stilt root cone that in
171 extreme cases may reach over 2 m in height (Avalos and Schneider 2011). Understory
172 species included *Prestoea decurrens*, *Chamaedorea tepejilote*, *Geonoma interrupta* and
173 *Asterogyne martiana*. *Prestoea decurrens* (Nicaragua to Ecuador, 0-900 masl), is a clonal
174 species reaching 10 m in height (Grayum 2003). *Chamaedorea tepejilote* (S Mexico to
175 Colombia, 0-1600 masl) is a dioecious species which can grow up to 5 m (Grayum 2003,
176 Castillo-Mont et al. 1994). *Geonoma interrupta* (S Mexico to Peru, 0-850 masl) has a
177 solitary stem and may reach 6 m in height (and over 10 m in exceptional cases), being
178 considered as one of the tallest species in the genus (Grayum 2003). Finally, *Asterogyne*
179 *martiana* (Belize to Ecuador, 0-1,000 masl) is an understory species with a decumbent stem
180 often reaching 2 m in height, and with simple, bifid leaves.
181
182 ***Palm harvesting, morphological measurements, and biomass estimation***
183 From Sept-2013 to May-2015, we harvested 87 palms, representing the full range of size
184 classes observed in the field (Table 1). We measured stem diameter at 1.3 m above the
185 ground, at half the stem length in palms less than 1.3 m in height, or immediately above the
186 stilt roots in palms with a stilt root cone higher than 1.3 m, and called this measurement in
187 all cases, DBH. Harvested palms were separated into modules (stems, roots, and leaves)
188 and we measured the total fresh biomass of each module using a Pesola® Macro-Line
189 Spring Scale (30 ± 0.25 kg). We dug out the roots carefully, collected all the root material
190 to the extent that was possible, including fine roots (5 mm in diameter). In instances in
191 which it was difficult to extract all the roots, due to their size or depth, a representative
192 section was extracted, and from this, we estimated the total root biomass. We washed out

193 the roots in the field and sun-dried them before weighing them in the laboratory. To
194 determine the dry biomass (and carbon content) we collected 300 mg samples from each
195 module. For leaves this sample included one young, one intermediate, and one mature
196 frond, determined according to their position from the tip of the apical meristem. In stems,
197 the biomass sample was collected from the base, middle, and upper part of the stem until
198 reaching the base of the leaf crown. The total height of the palm (H_{tot}) was measured from
199 ground level to the base of the crown, including the height of the cone of stilt roots (if
200 present), or as the total length of the stem (from the point of connection with the roots to
201 the base of the petiole of the youngest leaf), including the section of the subterranean stem
202 in *A. martiana*. This measurement is more practical for forest inventories, since in a
203 complex forest it is difficult to observe the very top of the apical meristem within a dense
204 palm crown and a dense forest canopy. The height of the stem to the base of the crown
205 (H_{bc}) was estimated as the length of the aerial stem (from the top of the root cone if present,
206 that is, the base of the stem) to the insertion of the oldest leaf, which corresponds to the
207 base of the crown. This measurement was recorded for stilt rooted species (*S. exorrhiza*, *I.*
208 *deltoidea*, *E. precatoria*, and *P. decurrens*). Finally, to estimate the tissue density of the
209 stem (specific gravity, ρ), we used a Haglof 2-Thread Increment Borer, to collect a tissue
210 sample from the stem, following the methods of Chave et al. (2005). Accordingly, we
211 selected a point of entry for the increment borer near the base of the stem, in the middle,
212 and near the base of the palm crown to place the borer at the center of the internode and
213 carry out the perforation. Once the sclerotized tissue was extracted, the sample was placed
214 in a test tube, sealed, and transferred back to the laboratory for the estimation of tissue
215 density.
216

Estimation of carbon content and stem tissue density

We dried the samples in an oven at 65°C for 48 h or until constant weight. Once dried, we ground the samples and determined their carbon content using an automatic analyzer TruSpec CN, LECO Corporation, at the Laboratory of the Department of Systematic Botany at the University of Ulm, Germany, and an automatic elemental carbon and nitrogen analyzer, VarioMacrocube, at the University of Costa Rica. The magnitude of the carbon content in g was calculated by multiplying the total dry weight of each module by the percentage of carbon obtained in the laboratory and adding up all the dry biomass per individual palm. The average carbon fraction for the palms analyzed here was 43.9% ± 1.28 (Cambronero et al. 2018), but for our models we used the average carbon fraction obtained for each species. Stem tissue density (specific gravity, ρ) was calculated as the ratio of dry biomass (g) over volume (cm^3). Volume was measured by water displacement.

Estimation of total leaf area per palm

To determine the total leaf area, we followed the methods of Avalos and Sylvester (2010). The three collected leaves (one young, one intermediate, and one mature), were cleaned with a dry cloth and the leaf area was measured with a LICOR LI-3100 C leaf area meter (LICOR, Lincoln, NE, USA). From these measurements we estimated the total leaf area per individual palm by averaging the leaf area of the three leaves and multiplying it by the total number of fronds. This parameter was not used to predict carbon accumulation since measuring leaf area is difficult in forest inventories. However, we included it in the principal component analysis to examine palm morphological variation across species.

Allometric equations for estimating carbon content

241 The generation of allometric models aims to provide practical options for applying them in
242 studies of forest carbon inventories. We proposed models including a combination of
243 variables that are commonly measured under field conditions, such as DBH and stem
244 height. We included stem tissue density to explore the importance of this parameter in
245 palms, although its measurement requires access to instrumentation that might not be
246 readily available in the field. To predict carbon content, we calculated linear and
247 logarithmic stepwise regressions between the natural logarithm of the total amount of
248 carbon content in kg per palm (LN (C), response variable), and a set of explanatory
249 variables including DBH (cm), total stem height from the base of the stem to the base of the
250 leaf crown (H_{tot}, m, including stilt roots if present), the height of the stem to the base of the
251 crown (H_{bc}, m, excluding stilt roots if present), the dry mass fraction (dry mass over fresh
252 mass, dmf), and stem tissue density (g cm^{-3}). The predictor variables were included in the
253 models with their ln-transformed values as well as in their linear scales. We carried out the
254 stepwise regression analysis for each species, and then selected the most parsimonious
255 general regression model for all seven species based on the magnitudes of the R^2 value, the
256 mean square of error (MSE), and the Akaike Information Criterion (AIC). Since the
257 response variable required a logarithmic transformation, a correction factor was calculated,
258 according to Sprugel (1983). We used R software for all statistical analyses. In cases where
259 a higher fit of the model was justified, we combined two or more predictor variables.
260
261 ***Estimation of above-ground carbon content in palms: comparing a pantropical tree***
262 ***model and a general palm model***
263 We estimated the aboveground carbon content (AGC in kg) by adding the carbon content
264 fractions of stems and leaves without considering the carbon content of roots to compare

265 our model with those of Goodman et al. (2013) and Chave et al. (2014), which consider
266 only above ground biomass (AGB). Goodman et al. (2013)´s model estimates AGB for 8
267 species of neotropical palms, including *E. precatoria*, *I. deltoidea* and *S. exorrhiza*,
268 examined here, using $AGB^{0.25} = (dmfD^2H_{stem})^{0.25}$, where dmf is the dry mass fraction
269 defined above, D is DBH, and H_{stem} is the height of the palm from the ground to the highest
270 leaf. To determine AGC, we applied the conversion factor of 50% of the dry biomass,
271 which has traditionally been used to determine the carbon accumulated in trees (Chave et
272 al. 2005; Houghton 2007; Lorenz and Lal 2010). The pantropical model of Chave et al.
273 (2014) estimates AGB using $0.0673(\rho D^2H)^{0.976}$, where ρ corresponds to wood stem density
274 (g cm^{-3}, or tissue density for palms), D is the DBH (cm), and H is the total height (m); this
275 model is based on data from 4,004 trees ≥ 5 cm. AGC was then calculated by applying the
276 carbon fraction of 50% to AGB as in the case of Goodman et al. (2013)´s model. We did
277 not include other models developed for palms such as the one by Brown (1997), or by
278 Frangi and Lugo (1985), since these had lower performance and lower R^2 values when
279 applied to our data (0.78 and 0.79, respectively).
280 We used the actual carbon fraction per palm species measured directly here
281 (Cambronero et al. 2018) for the comparison with Goodman et al. (2013) and Chave et al.
282 (2014) models. In both cases, the accuracy of all models was contrasted against the
283 observed values of AGC using the R^2 value and the magnitude of their residuals. We used
284 natural logarithmic models for the comparisons.
285 ***Root:shoot ratios***
286 We calculated root:shoot ratios as the dry biomass of roots over the dry biomass of above-
287 ground parts (stems and leaves). This corresponds to the root:shoot ratio of dry biomass. In

288 addition, we obtained the root:shoot ratio of the carbon fraction after calculating the carbon
289 fraction of the above-ground and below-ground biomass.
290
291 ***Analysis of the correlation structure of morphological characters in our subset of palms***
292 We analyzed interspecific variation in key individual morphological traits related to
293 biomass allocation and tissue quality: tissue density, dmf, slenderness ratio (total stem
294 height over DBH), and root:shoot ratios (calculated based on the dry biomass, and carbon
295 content levels). We measured the phenotypic variation in morphological characters using
296 the ln-transformation of DBH, stem height, number of leaves, tissue density, dmf, leaf area,
297 slenderness ratio, root:shoot ratio (at the biomass and carbon content level), and total stored
298 carbon through principal component analysis, and used the scores of the first two
299 components to inspect the distribution of all the species in the multidimensional space
300 defined by correlation structure of morphological characters.
301
302 **Results**
303 Palms across species showed a wide range of sizes, reflecting the variation observed in the
304 field, where size and biomass increased from understory to canopy species (Table 1).
305 Average tissue density differed among canopy and subcanopy species (lower values) vs.
306 understory species (higher values, $F_{6,80} = 8.44$, $P < 0.0001$). Tissue density decreased from
307 canopy to understory species, but understory species showed higher variation (Figure 1A).
308 Differences in tissue density were significant among species (2-way ANOVA, $F_{2,221} =$
309 62.86, $p < 0.0001$), and position along the stem ($F_{6,221} = 3.94$, $p = 0.02$). Even though tissue
310 density varied with position in the stem (Figure 2), the magnitude of the differences was

311 small within a species. Therefore, we used the average value of tissue density as a predictor
312 of carbon content in our models.
313 There were significant differences in slenderness ratio across species ($F_{6,80}$ = 6.95, P
314 < 0.0001). Differences were not associated with strata, but were centered among species,
315 with *E. precatoria*, *P. decurrens* and *G. interrupta* showing the highest values (Figure 1B).
316 The dmf ratio also showed significant differences among species ($F_{6.80}$ = 16.2, P < 0.001,
317 Figure 1C). Here, differences followed the strata, with understory species showing highest
318 dmf values. Root:shoot ratios measured at the dry biomass level also showed significant
319 differences among species ($F_{6,80}$ = 4.92, P = 0.0002, Figure 1D), with *S. exorrhiza* and *A.*
320 *martiana* showing the highest values. The same pattern was found when the analysis was
321 done for root:shoot ratios based on carbon content ($F_{6,80}$ = 5.25, P = 0.0001, Figure 1E).
322 Here, *S. exorrhiza* diverged from the rest, which had small differences in this parameter
323 across species.
324
325 ***Species-level allometric models to estimate total carbon content.***
326 ***Canopy and subcanopy species***
327 In *S. exorrhiza* the most parsimonious model for predicting total carbon content had the
328 linear form of DBH. Entering other variables in the model (total height and stem height
329 from the base, in linear and logarithmic forms -in addition to Ln(DBH)-), produced similar
330 R^2 values but not a lower AIC (Table 2). For *I. deltoidea*, the most parsimonious models
331 included DBH and total height, both in its logarithmic and linear forms. For the subcanopy
332 palm, *E. precatoria*, the most parsimonious models had total height, height from the base of
333 the stem, and DBH (linear and logarithmic), with the linear form of total height as the best-
334 fit model. In none of the canopy and subcanopy species, tissue density and dmf had a

335 significant effect on carbon content (Table 2). In this set of species, R^2 values from
336 significant regressions were high and ranged from 0.79 to 0.97. Models combining two or
337 more predictor variables produced a fit comparable to the highest value of R^2 of single-
338 variable models. Models combining two or more variables were not considered as optimal
339 since it was not justified to increase model complexity without a significant change in the
340 fit of the model.
341
342 ***Understory species***
343 Understory species showed a lower fit relative to canopy and subcanopy species, with R^2
344 values ranging from 0.28 to 0.95. For *C. tepejilote*, we did not find differences in the
345 morphological parameters among male and female plants, and thus, the analyses were done
346 for the overall species. The best-fit model included the logarithmic form of total height and
347 DBH. For *P. decurrens*, the logarithmic forms of height from the base of the stem and total
348 height were the most parsimonious models, with similar R^2 values (0.85-0.87) for models
349 with one variable. The combined model for *P. decurrens* included the ln-transformations of
350 DBH, total height, and tissue density, with an R^2 value of 0.95. For *A. martiana*, the most
351 efficient models had DBH as the best predictor variable, both in its linear and logarithmic
352 forms. The most parsimonious model in this species, however, had the logarithmic forms of
353 DBH and tissue density. Finally, *G. interrupta* showed the highest fit for models including
354 total height (logarithmic and linear, with a R^2 of 0.92 and 0.91, respectively) as the most
355 parsimonious. In this species, DBH did not influence carbon content. *Prestoea decurrens*
356 and *G. interrupta* were the species for which tissue density had a significant effect on
357 carbon content (Table 2). Dry mass fraction had a significant effect on carbon storage only
358 in *G. interrupta*.

359

360 ***Family-level model to estimate total carbon content and above-ground carbon content***

361 The total height and DBH (both in linear and logarithmic forms) generated the models with
362 low AIC values to estimate total carbon content at the family level (Ln(C), Table 3). To
363 these variables, we added dmf to generate a general natural logarithmic model explaining
364 92% of the variation in stored carbon across species; this model had the lowest AIC value
365 (Table 3). The models that were significant and included a single variable ranged in R^2
366 values from 0.66 (DBH) to 0.80 (Ln H_{tot} and linear H_{tot}). Tissue density was not significant.
367 The variable dmf had a significant effect although the amount of variation explained in total
368 carbon content was low.

369 We followed a similar procedure to estimate AGC (Table 4). The most
370 parsimonious model (highest R^2, 0.91, and lowest AIC, -107.05) had the logarithmic
371 transformation of DBH, total height, and dmf as predictors of Ln (AGC).

372 We then compared the most parsimonious model of Table 4 with the palm model of
373 Goodman et al. (2013) and the pantropical model proposed by Chave et al. (2014) for
374 dicotyledonous trees (Figure 3) using Ln (AGC). All three models predicted the observed
375 Ln (AGC) with high R^2 values ranging from 0.879-0.911. Our model had the highest R^2
376 value (0.911) followed by Chave et al. (2014) with 0.882, and then Goodman et al. (2013)´s
377 with 0.879. Chave et al. (2014)´s model showed the highest residual variation, and
378 Goodman et al. (2013) the lowest. We consider all three models to be sufficiently efficient
379 to predict the AGC of the palm species analyzed here.

380

381 ***Principal component analysis***

382 The correlation matrix of morphological characters showed higher and positive correlation
383 coefficients among variables related to palm size, such as DBH, H_{tot}, total carbon content,
384 and leaf area. Variables related to structural characteristics, such as slenderness ratio, tissue
385 density, and root:shoot ratios, had low correlation coefficients (Figure 4). The variable dmf
386 showed intermediate correlation values.

387 We defined three principal components explaining 77.87% of the variation in the
388 data. The first component (44.4%) had a similar weight of DBH, height, and total carbon
389 content, which were variables related to palm size. The second component (17.74%) had a
390 similar contribution of tissue density and slenderness ratio. The third component (15.73%)
391 had a similar contribution of root:shoot ratios, both based on total dry biomass and carbon
392 content (Table 5).

393 The distribution of species in the multidimensional space defined by the first two
394 principal components showed that understory species were more related to palm structure
395 and biomass distribution (tissue density, slenderness ratio and dmf), whereas subcanopy
396 and canopy species were more associated with characters related to palm size (DBH, stem
397 height, leaf area, total carbon content), as well as root:shoot ratios (Figure 5). Understory
398 species showed more spread of the data reflecting the high structural diversity found in this
399 group.

400

401 **Discussion**

402 The contribution of palms to overall forest biomass in neotropical rainforests is
403 small. On Barro Colorado Island, palms represented 0.43% of AGC (50-ha plot census
404 from 1982, pers. obs.). At the Luquillo tropical rainforest in Puerto Rico, which is
405 dominated by *Prestoea montana*, palms contribute 10.9% of the biomass (Frangi and Lugo

406 1985) and 32% of the fallen leaves. In the tropical rainforest of La Selva Biological Station
407 in Costa Rica, palms represented 5.4% of AGB, although they make up 25% of stems ≥ 10
408 cm DBH (Clark and Clark 2000). In Manaus, Brazil, stemless palms contributed 0.3% of
409 AGB (Nascimento and Laurance 2002). In a tropical rainforest, also in Manaus, palm
410 biomass represented, on average, less than 1% of the living AGB, although in some plots
411 they contributed 10% (de Castilho et al. 2006). In the upper Rio Negro basin, palms make
412 up 2.8% of AGB (Lima et al. 2012). In wetlands, palms may constitute a larger percentage
413 of AGB since in these environments they are often the dominant group and are established
414 on soils storing large amounts of carbon (Lähteenoja et al. 2009). Although palms make up
415 a small percentage of the carbon stock of neotropical rainforests, they are functionally
416 important (Boukili and Chazdon 2017), intervening in nutrient cycling (Fauset et al. 2015)
417 and food webs (Zona and Henderson 1989), and their abundance varies with topography
418 and edaphic conditions, and are dominating elements in wetlands (Myers 2013).
419 Nonetheless, developing allometric models specific for palms will increase the accuracy of
420 the estimates of carbon stocks of tropical forests, since it is necessary to refine the models
421 currently in use to include other life forms (e.g., lianas, epiphytes, tree ferns), which
422 although they are not as abundant as trees, have relevant ecological roles and vary their
423 abundance according to forest type, elevation, and edaphic factors.

424 Allometric analyses integrating palm biomass in studies of carbon stocks in tropical
425 forests remain scarce (but see Nascimento and Laurance 2002; Lima et al. 2012). The
426 accuracy of the allometric models obtained for the family Arecaceae would depend on the
427 species composition of the palms included in the model. As of today, family-level models
428 proposed for Arecaceae are based on a small number of species, showing a limited tribe
429 representation and a relatively limited range of sizes and number of harvested individuals

(i.e., Goodman et al. 2013; and this study). Many canopy palms frequently show heights above or below those included in these models. Harvesting large individuals is difficult, and many field sites do not allow it. In addition to sample size bias, allometric relationships change geographically due to environmental conditions (Avalos et al. 2019), like topography, edaphic factors, successional stage, climate, and nutrient availability (Eiserhardt et al. 2011).

The accuracy of allometric models is hampered by an incomplete inventory of functional characters for tropical plants, and especially for palms. Functional characters like tissue density (Rich 1986, 1987), dmf, slenderness ratio, leaf toughness, and SLA, and even stem height, as well as gas exchange characters, are rarely documented for palms as a group, or are limited to individual species (i.e., Araus and Hogan 1994; da Silva et al. 2015; Renninger and Phillips 2016). Much less is known about how these characters vary with ontogenetic stage and palm size (but see Chazdon 1986a, 1986b). Tissue density, for instance, varied with position along the stem as observed here, since sclerotized tissue is denser closer to the base and periphery of the stem, and decreases in abundance close to the top of the stem (Niklas 1992). The functional character databases are still data-deficient for palms, and for tropical species in general, although Kissling et al. (2019) provide a very comprehensive compilation. Still, these databases are based on a few individuals (e.g., http://db.worldagroforestry.org), and often do not provide metadata. It is necessary to incorporate more species, a larger sample size per species, a greater range of sizes, and phylogenetic bias corrections. In addition, many tropical habitats where palms are very abundant and dominant (Myers 2013) are not regularly inventoried for carbon stocks.

Despite these limitations, our classification of palms into forest strata showed a clear segregation in structure between understory, subcanopy, and canopy species, as

deduced from the principal component analysis. Understory species leaned towards characters reflecting biomass allocation such as slenderness value, dmf, and tissue density, whereas subcanopy and canopy species were associated with characters related to overall palm size, such as DBH, total height and leaf area, although shoot:root ratios also influenced their allometric strategy. Palms in general have higher slenderness ratio than dicotyledonous trees (Niklas et al. 2006). Many understory palms display their leaf area with a high degree of efficiency by reducing leaf overlap and increasing light interception (Takenaka et al. 2001; Alvarez-Clare and Avalos 2007). Shade-adapted palms can complete their life cycle and reproduce in the understory, despite growing very slowly (Chazdon 1986b; Sylvester and Avalos 2013), but when light conditions improve, they can opportunistically increase their growth and reproductive performance (Chazdon 1986a; Gatti et al. 2011). For understory palms, resource allocation has a higher selective value, and once they surpass a height threshold and have more access to light, the selective advantage is to maintain high resource acquisition by increasing in size, which was the strategy of sub-canopy and canopy species. The ample morphological variation shown in the space defined by the first two principal components demonstrates these general trends and illustrates the diversity of allometric strategies within understory and canopy species.

Functional characters such as dmf and tissue density showed a relatively high correlation coefficient (0.37), but their influence predicting carbon content was significant only in *G. interrupta*. Tissue density was not important in predicting carbon content for the rest of the species. A similar conclusion was reached by Goodman et al. (2013), although they did not measure tissue density directly and obtained their values from online databases. Dmf and tissue density were also correlated in Goodman et al. (2013)´s palm assemblage, and ultimately improved their mixed species model estimates of AGB. We

found significant but small differences in tissue density depending on stem position, and lower tissue density in canopy species relative to understory species. Chave et al. (2014)´s model incorporated wood density, and once we applied this model to our subset of palm species, the results were practically equivalent to the general palm model generated here. The relative high fit of the Chave et al. (2014) model to our data could have been influenced by having many palm species with a significant DBH vs. height relationship. Consequently, the model of Chave et al. (2014) did not overestimate palm carbon content in this case.

For most palms for which we have allometry data, there was a significant relationship between DBH and stem height (Avalos et al. 2019). However, this relationship is dependent on the palm species and phylogenetic relationships. It is erroneous to assume that all palms have a fixed and decoupled relationship between DBH and stem height, a view that is often prevalent in the literature (e.g., Tregear et al. 2011; Muscarella et al. 2020). Instead, some palm species could gradually increase DBH as they increase in height through sustained primary growth (i.e., through the division, lignification, and expansion of parenchyma cells, which can also differentiate into fibers, Tomlinson 2006, 2011), whereas others must create sufficient DBH support early in life before increasing in height. Usually, the relationship between DBH and stem height is logarithmic. In some species the relationship is strong (e.g., *S. exorrhiza*, *I. deltoidea*, *E. precatoria*, *P. decurrens*), in others it is intermediate (e.g., *G. interrupta*, $R^2 = 0.42$, $P = 0.04$, $N = 10$, Avalos et al. 2019), and finally, some species do not show a significant relationship (e.g., *M. flexuosa*, Goodman et al. 2013).

The diversity of palm growth forms (arborescent, acaulescent, climbing) makes it difficult to standardize data collection to generate family-specific allometric models. For

instance, we measured the total stem height from the ground to the base of the leaf crown, whereas in other studies (e.g., Goodman et al. 2013; Chave et al. 2014), total stem height was measured from the ground to the highest point of the plant, which may include the last leaf, with or without stilt roots, if present. We measured AGB from the base of the stem to the apex of the meristem, without including the cone of stilt roots; this cone is produced above the ground but was instead considered part of the below-ground biomass. Similarly, in *A. martiana* part of the stem grows underground, but we considered it as part of AGB. Dioecious palms, like *C. tepejilote*, may differ in biomass allocation between sexes, which was the case for in the study of Oyama and Dirzo (1988), although they harvested 15 individuals, including male and female plants, and juveniles. In our case, we did not find differences in allometric patterns between male and female plants and juveniles. Oyama and Dirzo (1988)´s study was based on the follow up of 810 individuals in a more comprehensive demographic study. In other studies, stem height is not measured directly but inferred from species descriptions (de Castilho et al. 2006). Although there are efforts to standardize the measurement of functional characters (e.g., Perez-Harguindeguy et al. 2013), these are still focused on woody plants and do not consider the structural and morphological diversity of other plant groups.

Estimation of root biomass and carbon content

Estimation of root biomass and carbon content continue to be a major gap in palm allometric analyses. The data is still fragmentary and often restricted to a few individual species (e.g., Goodman et al. 2013; da Silva et al. 2015), hence much of the information is concentrated on aerial biomass. The functional ecology of roots is still poorly understood in general, especially with regards to the integration of above and below-ground characters.

For example, leaf life span does not correlate with fine root longevity when resources are limited (Weemstra et al. 2016). Under these conditions, leaves with long lifespans are favored, but fine roots, responsible for increasing surface area and absorption capacity, show a high turnover rate. Future research should be focused on analyzing the level of integration between above and below-ground functional traits (Laliberté 2017). In our case, similarly to other studies trying to estimate root biomass (e.g., da Silva et al. 2015), it was difficult to obtain all roots, especially fine roots. Many palm species have superficial roots, which may explain their predominance in flooded environments and very wet forests, which are rich in palm species or are dominated by one or two species, since shallow roots fare better in wet environments (Eiserhardt et al. 2011). There are very few studies estimating root biomass for palms in the tropics (Frangi and Lugo 1985), so that comparative information is difficult to come by, although da Silva et al. (2015) report the same root:shoot ratio for *E. precatoria* found here.

Conclusions

After Goodman et al. (2013), this is the only recent study that has proposed a family-level model to estimate not only AGC but also the total carbon content per individual for the family Arecaceae. In addition to this model, we provided individual models for 7 of the most common and abundant palm species in tropical rainforests and estimated their below-ground biomass. Allometric models could have a high degree of complexity by including many variables as well as a varied combination of them. Our objective here was to simplify the selection of allometric models with practical importance for forest inventories, as well as to explore the role of morphological variables on carbon storage without proposing complex variable combinations. Most of the models that were

statistically significant had a logarithmic form, which is consistent with the functional relationship between allometric characters, such as DBH, stem height, and other traits related to palm size. It is necessary to include more species, a greater diversity of growth forms, a greater range of sizes, and larger sample size to improve the accuracy of allometric models in general, and for palms in particular. Palm species dominating wetlands continue to be deficient in this regard; despite dominating carbon-rich environments, there are few studies that include them, possibly due to the logistical difficulties of doing research in flooded environments. Finally, a better standardization of data collection is required to make progress in the estimation of carbon content using allometric methods, which continue to be a viable and efficient alternative to estimate carbon stocks.

Acknowledgements

Orlando Vargas facilitated field work at La Selva. Juan Manuel Ley facilitated field work at Tirimbina. Nutrient analyses were facilitated by Floria Bertsch at the Centro de Investigaciones Agronómicas, University of Costa Rica, and by Steven Jansen at the Department of Systematic Botany and Ecology, University of Ulm. The Alpízar Chaves family of El Progreso facilitated work in their property.

Funding: This investigation was supported by a research grant from the International Palm Society to MC, and scholarships from the Organization for Tropical Studies (MC and CAV), the University of Costa Rica (MC), and Tirimbina Biological Reserve (CAV). The School for Field Studies provided logistic support.

Ethics approval: The Ministry of the Environment of Costa Rica granted the respective research permits to carry out this research.

Availability of data and materials: The datasets used and/or analyzed during the current study are available from the corresponding author on reasonable request.

References

Achard F, Eva HD, Mayaux P, Stibig HJ, Belward A (2004) Improved estimates of net carbon emissions from land cover change in the tropics for the 1990's. Global Biobeochem Cy 18:1-11 doi:10.1029/2003GB002142

Araus JL, Hogan KP (1994) Leaf structure and patterns of photoinhibition in two neotropical palms in clearings and forest understory during the dry season. Am J Bot 81:726-738 doi: 10.1002/j.1537-2197.1994.tb15507.x

Ares A, Boniche J, Quesada JP, Yost R, Molina E, Smyth TJ (2002) Estimación de biomasa por métodos alométricos, nutrimentos y carbón en plantaciones de palmito en Costa Rica. Agron Costarric 26:19-30

Avalos G, Schneider R (2011) Quantification of ramet production in the neotropical palm *Euterpe precatoria* (Arecaceae) in Costa Rica. Ecotropica 17:95-102

Avalos G, Gei M, Ríos LD, Otárola MF, Cambronero M, Alvarez-Vergnan C, Sylvester O, Rojas G (2019) Scaling of stem diameter and height allometry in 14 neotropical palm species of different forest strata. Oecologia 190(4):757-767 doi: 10.1007/s00442-019-04452-7

Baker WJ, Dransfield J (2016) Beyond Genera Palmarum: progress and prospects in palm systematics. Bot J Linn Soc 182:207-233 doi: 10.1111/boj.12401

Brando PM, Paolucci L, Ummenhofer CC, Ordway EM, Hartmann H, Cattau ME, ... Balch J (2019) Droughts, wildfires, and forest carbon cycling: A pantropical synthesis. Annu Rev Earth Pl Sc 47:555-581 doi: 10.1146/annurev-earth-082517-010235

Brown S (1997) Estimating biomass and biomass change of tropical forests: a primer. FAO Forestry Paper -134, Illinois

603 Cambronero M, Avalos G, Alvarez-Vergnani C (2018) Variation in the carbon fraction
604 of seven neotropical palm species of different forest strata. Palms 62(1):25-34.
605 Canadell JG, Raupach MR (2008) Managing forests for climate change mitigation.
606 Science 320:1456-1457 doi: 10.1126/science.1155458
607 Castillo-Mont JJ, Gallardo NR, Johnson DV (1994) The pacaya palm (*Chamaedorea*
608 *tepejilote*, Arecaceae) and its food use in Guatemala. Econ Bot 48:68-75 doi:
609 10.1007/BF02901383
610 Chave J, Andalo C, Brown S, Cairns MA, Chambers J Q, … Yamakura T (2005) Tree
611 allometry and improved estimation of carbon stocks and balance in tropical
612 forests. Oecologia 145:87-99 doi: 10.1007/s00442-005-0100-x
613 Chave J, Réjou-Méchain M, Búrquez A, Chidumayo E, Colgan M, Delitti W, …
614 Vieilledent G (2014) Improved allometric models to estimate the aboveground
615 biomass of tropical trees. Glob Change Biol 20:3177-3190 doi: 10.1111/gcb.12629
616 Chazdon RL (1986a) Light variation and carbon gain in rain forest understorey palms. J
617 Ecol 74:995-1012 doi: 10.2307/2260229
618 Chazdon RL (1986b) Physiological and morphological basis of shade tolerance in rain
619 forest understory palms. Principes 30:92-99
620 Clark DB, Clark DA (2000) Landscape-scale variation in forest structure and biomass in
621 a tropical rain forest. Forest Ecol Manag 137:185-198 doi: 10.1016/S0378-
622 1127(99)00327-8
623 Clark DA, Brown S, Kicklighter DW, Chambers JQ, Thomlinson JR, Ni J (2001)
624 Measuring net primary production in forests: Concepts and field methods. Ecol
625 Appl 11:356-370 doi: 10.1890/1051-0761(2001)011

626 Clark DA (2007) Detecting tropical forests' response to global climatic and atmospheric
627 change: current challenges and a way forward. Biotropica, 39:4-19 doi:
628 10.1111/j.1744-7429.2006.00227.x
629 Curtis PS (2008) Estimating aboveground carbon in live and standing dead trees. In:
630 Hoover CM (ed) Field measurements for forest carbon monitoring, a landscape-
631 scale approach. Springer, New York, pp 39-44
632 Da Silva F, Suwa R, Kajimoto T, Ishizuka M, Higuchi N, Kunert N (2015) Allometric
633 equations for estimating biomass of *Euterpe precatoria*, the most abundant palm
634 species in the Amazon. Forests 6:450-463 doi: 0.3390/f6020450
635 Dargie GC, Lewis SL, Lawson IT, Mitchard ET, Page SE, Bocko YE, Ifo SA (2017)
636 Age, extent and carbon storage of the central Congo Basin peatland complex.
637 Nature 542:86-90 doi: 10.1038/nature21048
638 de Castilho CV, Magnusson WE, de Araújo RNO, Luizao RC, Luizao FJ, Lima AP,
639 Higuchi N (2006) Variation in aboveground tree live biomass in a central
640 Amazonian Forest: Effects of soil and topography. Forest Ecol Manag 234:85-96
641 doi: 10.1016/j.foreco.2006.06.024
642 DeWalt SJ, Chave J (2004) Structure and biomass of four lowland Neotropical forests.
643 Biotropica 36:7-19 doi: 10.1111/j.1744-7429.2004.tb00291.x
644 Dewar RC (1991) Analytical model of carbon storage in the trees, soils and wood
645 products of managed forests. Tree Physiology 8:239-258 doi: 10.1111/j.1744-
646 7429.2004.tb00291.x
647 Dewar RC, Cannell MGR (1992) Carbon sequestration in the trees, products and soils of
648 forest plantations using UK samples. Tree Physiol 11:49-71 doi:
649 10.1093/treephys/11.1.49

650 Díaz S, Settel J, Brondízio ES, Ngo HT, Guèze M, Agard J, ... Zayas C (2019) Summary
651 for policymakers of the global assessment report on biodiversity and ecosystem
652 services of the Intergovernmental Science-Policy Platform on Biodiversity and
653 Ecosystem Services. Intergovernmental Science-Policy Platform on Biodiversity
654 and Ecosystem Services
655 Dransfield JN, Uhl W, Amussen CB, Baker WHJ, Harley MM, Lewis CE (2008) Genera
656 Palmarum: the evolution and classification of palms. London, Kew Publishing
657 Royal Botanic Gardens
658 Eiserhardt WL, Svenning JC, Kissling WD, Balslev H (2011) Geographical ecology of
659 the palms (Arecaceae): determinants of diversity and distributions across spatial
660 scales. Ann Bot 108:1391-1416 doi: 10.1093/aob/mcr146
661 Ekadinata AE, Khasanah N, Rahayu S, Budidarsono S, van Noordwijk M (2010) Carbon
662 footprint of Indonesian palm oil production: sample design and methodology.
663 World Agroforestry Centre, International Centre for Research in Agroforestry,
664 Indonesia
665 Fauset S, Johnson MO, Gloor M, Baker TR, Monteagudo A, Brienen RJ, ... Phillips OL
666 (2015) Hyperdominance in Amazonian forest carbon cycling. Nat Commun 61-9.
667 doi:10.1038/ncomms7857
668 Feldpausch TR, Banin L, Phillips OL, Baker TR, Lewis SL, Quesada CA, ... Lloyd J
669 (2011) Height-diameter allometry of tropical forest trees. Biogeosciences 8:1081-
670 1106 doi: 10.5194/bg-8-1081-2011
671 Frangi JL, Lugo AE (1985) Ecosystem dynamics of a subtropical floodplain forest. Ecol
672 Monogr 55:351–369 doi: 10.2307/1942582

673 Friedlingstein P, O'Sullivan M, Jones MW, Andrew RM, Hauck J, Olsen A, ... Zaehle S
674 (2020) Global carbon budget 2020. Earth Sys Sci Data 12:3269-3340 doi:
675 10.5194/essd-12-3269-2020
676 Gatti MG, Campanello PI, Goldstein G (2011) Growth and leaf production in the
677 tropical palm *Euterpe edulis*: Light conditions versus developmental constraints.
678 Flora-Morphology, Distribution, Functional Ecology of Plants 206:742-748 doi:
679 10.1016/j.flora.2011.04.004
680 Goers L, Ashton MS, Tyrrell ML (2012) Introduction. In: Ashton MS, Tyrrell ML,
681 Spalding D, Gentry B (eds) Managing forest carbon in a changing climate.
682 Springer, Netherlands pp 1-4
683 Goodman R, Phillips OL, Torres D, Freitas L, Tapia-Cortese S, Monteagudo A, Baker T
684 (2013) Amazon palm biomass and allometry. Forest Ecol Manag 310:994-1004
685 doi: 10.1016/j.foreco.2013.09.045
686 Grayum MH (2003) Arecaceae. In: Hammel BE, Grayum MH, Herrera C, Zamora N
687 (eds), Manual de Plantas de Costa Rica, Vol. III. Missouri Botanical Garden, St.
688 Louis pp 201-293
689 Hairiah K, Sitompul SM, van Noordwijk M, Palm C (2001) Methods for sampling
690 carbon stocks above and below ground. International Centre for Research in
691 Agroforestry, Southeast Asian Regional Research Programme, Indonesia
692 Henderson A (1995) The palms of the Amazon. Oxford University Press, New York
693 Henderson A, Galeano G, Bernal R (1995) Field guide to the Palms of the Americas.
694 Princeton University Press, New York
695 Henderson A (2002) Evolution and ecology of palms. New York Botanical Garden, New
696 York

697 Houghton RA (2007) Balancing the global carbon budget. Annu Rev Earth Pl Sc
698 35:313-347 doi: 10.1146/annurev.earth.35.031306.140057
699 Howard FW, Moore D, Giblin-Davis RM, Abad RG (2001) Insects on palms. CABI
700 Publishing ,Wallingford
701 Jones DL (1995) Palms throughout the world. Smithsonian Institution Press,
702 Washington DC
703 Jucker T, Caspersen J, Chave J, Antin C, Barbier N, Bongers F, ... Coomes DA (2017)
704 Allometric equations for integrating remote sensing imagery into forest monitoring
705 programmes. Glob Change Biol 23:177-190 doi: 10.1111/gcb.13388
706 Khasanah N, van Noordwijk M, Ekadinata A, Dewi S, Rahayu S, Ningsih H, …
707 Octaviani R (2012) The carbon footprint of Indonesian palm oil production.
708 (Technical Brief No 25: Palm oil series). World Agroforestry Centre - ICRAF,
709 SEA Regional Office, Indonesia
710 Kissling WD, Balslev H, Baker WJ, Dransfield J, Göldel B, Lim JY, ... Svenning JC
711 (2019) PalmTraits 1.0, a species-level functional trait database of palms
712 worldwide. Sci Data 6:1-13 doi: 10.1038/s41597-019-0189-0
713 Lähteenoja O, Ruokolainen K, Schulman L, Oinonen M (2009) Amazonian peatlands:
714 an ignored C sink and potential source. Glob Change Biol 15:2311-2320 doi:
715 10.1111/j.1365-2486.2009.01920.x
716 Lal R (2008) Carbon sequestration. Philos T Roy Soc B 363:815-830 doi:
717 10.1098/rstb.2007.2185
718 Laliberté E (2017) Below-ground frontiers in trait-based plant ecology. New Phytol
719 213:1597-1603 doi: 10.1111/nph.14247

720 Leblanc H, Russo R, Cueva JJ, Subía E (2006) Fijación de carbono en palma aceitera en
721 la región tropical húmeda de Costa Rica. Tierra Tropical 2:197-202
722 LECO Corporation (2006) TruSpec CN Carbon/Nitrogen determinator, instruction
723 manual. Software version 1.6x. LECO Corporation, Miami
724 Lima AJN, Suwa R, de Mello Ribeiro GHP, Kajimoto T, dos Santos J, da Silva RP, ...
725 Higuchi N (2012) Allometric models for estimating above-and below-ground
726 biomass in Amazonian forests at São Gabriel da Cachoeira in the upper Rio Negro,
727 Brazil. Forest Ecol Manag 277:163-172 doi: 10.1016/j.foreco.2012.04.028
728 Lorenz K, Lal R (2010) Carbon sequestration in forest ecosystems. Springer Verlag,
729 Berlin
730 McDade LA (1994) La Selva: Ecology and natural history of a neotropical rainforest.
731 University of Chicago Press, Chicago
732 Mejia K, Kahn F (1990) Palm Communities in Wetland Forest Ecosystems of Peruvian
733 Amazonia. Forest Ecol Manag 33–34:169-179 doi: 10.1016/0378-1127(90)90191-
734 D
735 Montero M, Montagnini F (2005) Modelos alométricos para la estimación de biomasa de
736 diez especies nativas en plantaciones en la región Atlántica de Costa Rica.
737 Recursos Naturales y Ambiente 45:112-119
738 Myers RL (2013) Humedales dominados por palmas (Arecaceae) en el Neotrópico: Una
739 introducción. Rev Biol Trop 61:5-24
740 Muscarella R, Emilio T, Phillips OL, Lewis SL, Slik F, Baker WJ, ... Poedjirahajoe E
741 (2020) The global abundance of tree palms. Glob Ecol Biogeogr 29:1495-1514
742 doi: 10.1111/geb.13123

743 Nascimento HE, Laurance WF (2002) Total aboveground biomass in central Amazonian
744 rainforests: a landscape-scale study. Forest Ecol Manag 168:311-321 doi:
745 10.1016/S0378-1127(01)00749-6
746 Niklas KJ (1992) Plant biomechanics: an engineering approach to plant form and
747 function. The University of Chicago Press, Chicago
748 Niklas KJ, Cobb ED, Marler T (2006) A comparison between the record height-to-stem
749 diameter allometries of pachycaulis and leptocaulis species. Ann Bot 97:79-83 doi:
750 10.1093/aob/mcj002
751 Onstein RE, Baker WJ, Couvreur TL, Faurby S, Svenning JC, Kissling WD (2017)
752 Frugivory-related traits promote speciation of tropical palms. Nat Ecol Evol
753 1:1903-1911 doi: 10.1038/s41559-017-0348-7
754 Oyama K, Dirzo R (1988) Biomass allocation in the dioecious tropical palm
755 *Chamaedorea tepejilote* and its life history consequences. Plant Spec Biol 3:27-33
756 doi: 10.1111/j.1442-1984.1988.tb00168.x
757 Perez-Harguindeguy N, Diaz S, Garnier E, Lavorel S, Poorter H, Jaureguiberry P, ...
758 Cornelissen JHC (2013) New handbook for standardised measurement of plant
759 functional traits worldwide. Aust. Bot. 61:167–234. doi: 10.1071/BT12225
760 Pulhin FB, Lasco RD, Urquiola JP (2014) Carbon sequestration potential of oil palm in
761 Bohol, Philippines. Ecosystems & Development Journal 4:14-19
762 Renninger HJ, Phillips NG (2016) Palm physiology and distribution in response to
763 global environmental change. In: Goldstein G, Santiago LS (eds), Tropical Tree
764 Physiology. Springer, Switzerland, pp 67-101
765 Rich P (1986) Mechanical architecture of arborescent rain forest palms. Principes
766 30:117-131

767 Rich PM (1987) Mechanical structure of the stem of arborescent palms. Bot Gaz 148:42-
768 50.
769 Rodríguez-Veiga P, Quegan S, Carreiras J, Persson HJ, Fransson JE, Hoscilo A, ...
770 Balzter H (2019) Forest biomass retrieval approaches from earth observation in
771 different biomes. Int J Appl Earth Obs 77:53-68. doi: 10.1016/j.jag.2018.12.008
772 Sampaio MB, Schmidt IB, Figueiredo IB (2008) Harvesting effects and population
773 ecology of the buriti palm (*Mauritia flexuosa* L. f., Arecaceae) in the Jalapão
774 Region, Central Brazil. Econ Bot 62:171-181 doi: 10.1007/s12231-008-9017-8
775 Serrano-Sandí J, Bonilla-Murillo F, Sasa M (2013) Distribución, superficie y área
776 protegida de humedales dominados por pantanos de palmas (Arecaceae) en Costa
777 Rica y Nicaragua. Rev Biol Trop 61:25-33
778 Sprugel DG (1983) Correcting for bias Log-transformed allometric equations. Ecology
779 64:209-210 doi: 10.2307/1937343
780 Steffen W, Rockström J, Richardson K, Lenton TM, Folke C, Liverman D, ...
781 Schellnhuber HJ (2018) Trajectories of the Earth System in the Anthropocene.
782 Proc Natl Acad Sci USA 15:8252-8259 doi: 10.1073/pnas.1810141115
783 Syahrinudin (2005) The potential of oil palm and forest plantations for carbon
784 sequestration on degraded land in Indonesia. Ecology and Development Series 28,
785 Germany
786 Sylvester O, Avalos G, Chávez-Fernández N (2012) Notes on the ethnobotany of Costa
787 Rica's palms. Palms 56:190-201
788 Sylvester O, Avalos G (2013) Influence of light conditions on the allometry and growth
789 of the understory palm *Geonoma undata* subsp. *edulis* (Arecaceae) of neotropical
790 cloud forests. Am J Bot 100:1-7. doi: 10.3732/ajb.1300247

ter Steege H, Pitman NCA, Sabatier D, Baraloto C, Salomão RP, Guevara JE, … Silman MR (2013) Hyperdominance in the Amazonian tree flora. Science 342:325-342 doi: 10.1126/science.1243092

Thenkabail PS, Stucky N, Griscom BW, Ashton MS, Diels J, Van Der Meer B, Enclona E (2004) Biomass estimations and carbon stock calculations in the oil palm plantations of African derived savannas using IKONOS data. Int J Remote Sens 25:1-27 doi: 10.1080/01431160412331291279

Tomlinson PB (2006) The uniqueness of palms. Bot J Linn Soc 151:5-14 doi: 10.1111/j.1095-8339.2006.00520.x

Tomlinson PB (2011) The anatomy of palms. Oxford University Press, New York

Tregear JW, Rival A, Pintaud JC (2011) A family portrait: unravelling the complexities of palms. Ann Bot 108:1387-1389 doi: 10.1093/aob/mcr269

Weemstra M, Mommer L, Visser EJ, van Ruijven J, Kuyper TW, Mohren GM, Sterck FJ (2016) Towards a multidimensional root trait framework: a tree root review. New Phytol 211:1159-1169 doi: 10.1111/nph.14003

Yaap B, Watson H, Laurance WF (2015) Mammal use of *Raphia taedigera* palm stands in Costa Rica's Osa Peninsula. Mammalia 79:357-362 doi: 10.1515/mammalia-2014-0033

Zhang X, Zhao Y, Ashton MS, Lee X (2012) Measuring carbon in forests. In: Ashton MS, Tyrrell ML, Spalding D, Gentry B (eds), Managing forest carbon in a changing climate. Springer, Netherlands, pp 139-164

Zona S, Henderson A (1989) A review of animal-mediated seed dispersal of palms. Selbyana 11:6-21

Table 1. Summary of morphological variables of 7 palm species harvested in the Caribbean lowlands of Costa Rica to obtain allometric models to estimate carbon content and above ground biomass. Values correspond to means (minium-maximum values).

Species (Abbreviation)	Stratum	Tribe[1]	N	DBH (cm)	H (m)	Tissue density (g/cm^3)	Total dry biomass (kg)	AGB (kg)	Number of leaves	Leaf area (m^2)	Dry weight leaves (kg)	Dry weight stem (kg)	Dry weight roots (kg)	Carbon in leaves (kg)	Carbon in stems (kg)	Carbon in roots (kg)	Total carbon per palm (kg)	Root:shoot (carbon)	Root:shoot (biomass)
Asterogyne martiana (AM)	Understory	Geonomateae	15	2.5 (1.53-3.88)	0.78 (0.28 - 1.66)	0.35 (0.26-0.51)	0.3 (0.02 – 0.63)	0.05 (0.005-0.12)	9 to 26	1.17 (0.13-3.04)	0.10 (0.0003-0.29)	0.16 (0.005-0.4)	0.03 (0.002-0.08)	0.04 (0.005-0.13)	0.07 (0.002-0.18)	0.01 (0.001-0.03)	0.3 (0.02-0.63)	0.16 (0.032-0.36)	0.6 (0.11-2.54)
Chamaedorea tepejilote (CT)	Understory	Chamaedoreeae	22	3.04 (1.27-5.09)	2.82 (0.55- 6.72)	0.31 (0.14-0.6)	0.9 (0.05 – 2.93)	0.32 (0.01-1.2)	3 to 6	2.34 (0.22-4.65)	0.14 (0.02-0.34)	0.48 (0.01-2)	0.28 (0.006-1.14)	0.06 (0.02-0.15)	0.2 (0.006-0.89)	0.12 (0.003-0.51)	0.9 (0.04-2.93)	0.51 (0.10-2.54)	0.2 (0.03-0.76)
Prestoea decurrens (PD)	Understory	Euterpeae	10	6.74 (5.0 - 8.6)	6.31 (1.1 - 11.5)	0.34 (0.1-0.6)	9.16 (0.85-21.1)	2.88 (0.34-7.76)	5 to 12	8.8 (1.67-18.01)	3.8 (0.76-5.8)	11.34 (0.37-28.41)	5.57 (0.63-17.23)	1.64 (0.31-2.46)	4.92 (0.14-12.34)	2.6 (0.28-7.89)	9.15 (0.85-21.1)	0.40 (0.17-0.84)	0.38 (0.16-0.78)
Geonoma interrupta (GI)	Understory	Geonomateae	10	6.74 (5-8.6)	4.48 (0.69-11.62)	0.34 (0.16-0.48)	12.7 (0.4 – 54.51)	3.68 (0.2-14.53)	6 to 20	7.9 (1.58-25.04)	1.18 (0.14-5.16)	7.4 (0.23-32.68)	4.12 (0.02-19.64)	0.5 (0.06-2.21)	3.28 (0.08-14.66)	1.66 (0.01-6.66)	12.7 (0.4-54.51)	0.36 (0.07-0.56)	0.36 (0.07-0.56)
Euterpe precatoria (EP)	Subcanopy	Euterpeae	10	7.03 (3.5-12.8)	7.01 (2.2 - 12.6)	0.2 (0.15-0.26)	5.55 (0.36-27.14)	4.38 (0.33-14.75)	5 to 9	10.5 (2.6-28.66)	2.26 (0.57-10.1)	8.14 (0.08-42.97)	2.06 (0.08-7.89)	1.06 (0.26-4.78)	3.54 (0.03-18.75)	0.94 (0.03-3.59)	5.55 (0.36-27.14)	0.26 (0.02-1.28)	0.25 (0.02-1.24)
Iriartea deltoidea (ID)	Canopy	Iriarteeae	10	12.03 (4.4-23.6)	5.93 (1.0 - 11.5)	0.14 (0.08-0.2)	8.26 (0.22-28.46)	11.78 (0.24-39.17)	5 to 9	25.86 (2.63-79.66)	6.16 (0.34-20.92)	11.01 (0.07-41.94)	2.19 (0.07-8.82)	2.6 (0.14-9.0)	4.68 (0.02-17.84)	0.97 (0.03-3.84)	8.25 (0.22-28.46)	0.15 (0.02-0.36)	0.14 (0.01-0.31)
Socratea exorrhiza (SE)	Canopy	Iriarteeae	10	12.86 (2.4-20)	8.0 (1.4 - 14.8)	0.17 (0.09-0.38)	16.22 (0.09-58.06)	14.24 (0.11-34.64)	3 to 11	21.4 (1.28-53.31)	5.62 (0.08-15.96)	17.64 (0.02-63.19)	12.64 (0.11-49.16)	2.54 (0.04-7.25)	7.83 (0.008-28.62)	5.85 (0.05-22.92)	16.22 (0.09-58.06)	0.83 (0.31-1.9)	0.78 (0.31-1.7)

1 Follows Dransfield et al. (2008)

Table 2. Models to estimate carbon content (C; kg), in 7 species of neotropical palms. DBH: Diameter at breast height (cm), H_{tot}: Total height (m), H_{bc}: Height at the base of the crown (m), ρ: density of the sclerotized tissue (g/cm^3). CF: Correction factor recommended by Sprugel (1983). MSE: Mean square of error. AIC: Akaike's information criteria. Ln: Natural logarithm. The most parsimonious model is highlighted in bold-faced.

Species		Model	CF	R^2	F	P	MSE	AIC
Socratea exorrhiza	Ln(C)	-5.25 + 2.91 Ln(DBH)	1.01	0.92	101.8	<0.0001	2.56	-9.61
	Ln(C)	-2.71 + 2.43 $Ln(H_{tot})$	1.16	0.95	182.77	<0.0001	1.47	-15.14
	Ln(C)	-1.64 + 2.16 $Ln(H_{bc})$	1.16	0.94	126.52	<0.0001	2.09	-11.64
	Ln(C)	4.1 + 1.26 Ln(ρ)	n.s.	0.08	0.67	0.44	4.05	15.8
	Ln(C)	1.37 – 0.2 Ln(dmf)	n.s.	0.0009	0.03	0.94	4.4	16.56
	Ln(C)	**-2.6 + 0.34 DBH**	1.06	**0.97**	**280.74**	**<0.0001**	**0.97**	**-19.28**
	Ln(C)	-1.29 + 0.38 H_{tot}	1.3	0.88	57.37	<0.0001	0.54	-4.4
	Ln(C)	-1.1 + 0.44 H_{bc}	1.3	0.88	57.76	<0.0001	0.53	-4.49
	Ln(C)	0.3 + 8.49 ρ	n.s.	0.14	1.4	0.27	3.74	14.96
	Ln(C)	2.01 – 1.58 dmf	n.s.	0.001	0.0009	0.92	4.4	16.56
Combined model	**Ln(C)**	**-4.1 + 0.89 Ln(DBH) + 2.97 $Ln(H_{tot})$- 1.1 $Ln(H_{bc})$**	**1.06**	**0.97**	**65.35**	**<0.0001**	**0.17**	**-14.59**
Iriartea deltoidea	**Ln(C)**	**-4.43 + 2.48 Ln(DBH)**	**1.07**	**0.94**	**150.18**	**<0.0001**	**0.13**	**-18.16**
	Ln(C)	-1.64 + 1.92 $Ln(H_{tot})$	1.11	0.91	87.26	<0.0001	0.22	-13.18
	Ln(C)	-0.26 + 1.54 $Ln(H_{bc})$	1.25	0.83	40.12	0.0002	0.44	-6.26
	Ln(C)	-1.96 + 22.29 Ln(ρ)	n.s.	0.19	1.8	0.2	2.18	9.56

	Ln(C)	-3.96 – 2.62 Ln(dmf)	n.s.	0.21	2.22	0.17	2.1	9.22
	Ln(C)	-1.14 + 0.2 DBH	1.12	0.92	86.86	<0.0001	0.22	-13.06
	Ln(C)	-1.29 + 0.38 H_{tot}	1.19	0.94	129.88	<0.0001	0.16	-16.79
	Ln(C)	-0.68 + 0.53 $H_{bc)}$	1.3	0.8	32.85	0.0004	0.52	-4.6
	Ln(C)	-1.92 + 22.18 ρ	n.s.	0.28	3.2	0.11	1.92	8.29
	Ln(C)	3.78 - 17.86 dmf	n.s.	0.22	2.28	0.16	2.09	9.16
Combined model	**Ln(C)**	**-3.52 + 1.58 Ln(DBH) + 0.78 Ln(H_{tot})**	**1.04**	**0.97**	**116.9**	**<0.0001**	**0.08**	**-21.7**
Euterpe precatoria	Ln(C)	-1.49 + 0.37 Ln(DBH)	1.04	0.94	134.3	<0.0001	0.1	-21.5
	Ln(C)	-1.39 + 0.37 Ln($H_{tot)}$	1.08	0.90	77.94	<0.0001	0.16	-16.46
	Ln(C)	-0.77 + 0.38 Ln($H_{bc)}$	1.01	0.79	30.79	0.0005	0.36	-8.5
	Ln(C)	-1.57 + 13.69 ln(ρ)	n.s.	0.16	1.48	0.25	1.46	5.58
	Ln(C)	2.18 + 0.54 Ln(dmf)	n.s.	0.21	2.22	0.17	2.1	9.22
	Ln(C)	-1.5 + 0.38 DBH	1.06	0.93	114.86	<0.0001	0.11	-20.04
	Ln(C)	**-1.4+0.36 H_{tot}**	**1.04**	**0.95**	**161.26**	**<0.0001**	**0.08**	**-23.24**
	Ln(C)	-0.77 + 0.38 H_{bc}	1.06	0.93	109.96	<0.0001	0.94	-19.62
	Ln(C)	-1.6 + 13.91 ρ	n.s.	0.15	1.42	0.26	1.47	5.65
	Ln(C)	0.52 + 4.08 dmf	n.s.	0.22	2.28	0.16	2.09	9.16
Chamaedorea tepejilote	Ln(C)	-5.6 + 4 Ln(DBH)	1.02	0.66	38.59	<0.0001	0.41	-17.39
	Ln(C)	-2.4+ 1.29 Ln($H_{tot)}$	1.01	0.55	24.71	<0.0001	0.54	-11.45
	Ln(C)	-1.33+ 0.02 Ln(ρ)	n.s.	0.001	0.02	0.89	1.21	6.22

	Ln(C)	-0.68 + 0.49 Ln(dmf)	n.s.	0.01	0.36	0.55	1.2	5.84
	Ln(C)	-5.94 + 1.56 DBH	1.02	0.66	39.16	<0.0001	0.41	-17.6
	Ln(C)	-2.56 + 0.42 H_{tot}	1.03	0.76	65.22	0.0001	0.28	-25.64
	Ln(C)	-1.46 + 0.34 ρ	n.s.	0.	0.001	0.98	1.21	6.25
	Ln(C)	-1.72 + 1.36 dmf	n.s.	0.02	0.59	0.45	1.18	5.6
Combined model	**Ln(C)**	**-3.94 + 1.75 Ln(DBH) + 0.89 Ln(H_{tot})**	**1.02**	**0.81**	**43.79**	**<0.0001**	**0.23**	**-29.43**
Prestoea decurrens	Ln(C)	-8.67 + 5.58 Ln(DBH)	1.11	0.54	9.64	0.01	0.79	-0.57
	Ln(C)	-0.81 + 1.64 Ln(H_{tot})	1.02	0.86	51.66	<0.0001	0.23	-12.76
	Ln(C)	**-0.08 + 1.53 Ln(H_{bc})**	**1.05**	**0.87**	**55.06**	**0.0001**	**0.22**	**-13.31**
	Ln(C)	3.79 + 1.44 Ln(ρ)	1.22	0.76	25.96	0.0009	0.41	-7.12
		7.12 + 3.19 Ln(dmf)	n.s.	0.38	5.02	0.06	1.07	2.46
	Ln(C)	-3.65 + 0.82 DBH	1.5	0.53	9.14	0.01	0.81	-0.28
	Ln(C)	-0.27 + 0.34 H_{tot}	1.14	0.85	46.56	0.0001	0.26	-11.86
	Ln(C)	0.05 + 0.41 H_{bc}	1.21	0.78	28.3	0.0007	0.38	-7.78
	Ln(C)	0.18 + 5.05 ρ	1.27	0.72	20.9	0.001	0.48	-5.5
		-1.16 + 15.36 dmf	n.s.	0.38	4.82	0.06	1.08	2.61
Combined model	**Ln(C)**	**-1.5 + 1.92 Ln(DBH) + 0.56 Ln(H_{tot}) + 0.89 Ln(ρ)**	**1.04**	**0.95**	**91.63**	**0.0002**	**0.10**	**-19.49**
Asterogyne martiana	**Ln(C)**	**-5.21 + 3.27 Ln(DBH)**	**1.09**	**0.79**	**49.98**	**<0.0001**	**0.18**	**-23.53**

	Ln(C)	-1.87 + 1.08 $Ln(H_{tot})$	1.32	0.36	7.38	0.01	0.56	-6.61
	Ln(C)	-1.57 + 13.69 Ln(ρ)	n.s.	0.24	4.18	0.06	0.67	-4.04
	Ln(C)	Ln(dmf)	n.s.	0.03	0.44	0.51	0.86	-0.37
	Ln(C)	-5.79 + 1.4 DBH	1.12	0.73	35.56	<0.0001	0.24	-19.63
	Ln(C)	-3.22 + 1.22 H_{tot}	1.37	0.28	5.24	0.04	0.64	-4.94
	Ln(C)	-4.18 + 5.06 ρ	n.s.	0.23	3.94	0.06	0.68	-3.88
	Ln(C)	-0.87 – 4.4 dmf	n.s.	0.03	0.4	0.54	0.86	-0.32
Combined model	**Ln(C)**	**-3.85 + 3 Ln(DBH) + 1.06 Ln(ρ)**	**1.07**	**0.84**	**30.87**	**<0.0001**	**0.16**	**-25.09**
Geonoma interrupta	Ln(C)	-4.39 + 2.96 Ln(DBH)	n.s.	0.3	3.41	0.1	1.96	8.48
	Ln(C)	**-1.1 + 1.56 $Ln(H_{tot})$**	**1.1**	**0.92**	**105.44**	**<0.0001**	**0.2**	**-14.48**
	Ln(C)	5 + 3.82 Ln(ρ)	1.4	0.66	25.51	0.001	0.66	-2.28
		6.1 + 4.88 Ln(dmf)	1.26	0.83	40.22	0.0002	0.46	-5.92
	Ln(C)	-2.16 + 0.49 DBH	n.s.	0.33	4	0.08	1.86	7.97
	Ln(C)	-1.2 + 0.41 H_{tot}	1.13	0.91	83.58	<0.0001	0.24	-12.34
	Ln(C)	-3.68 + 12.8 ρ	1.33	0.79	30.88	0.0005	0.57	-3.78
	Ln(C)	-4.28 + 14.49 dmf	1.28	0.82	37.41	0.0003	0.49	-5.32

Table 3. General allometric models to estimate total carbon content (C; kg) based on 7 species of neotropical palms. DBH: Diameter at breast height (cm), H_{tot}: Total height (m), dmf: dry mass fracion, ρ: density of the sclerotized tissue (g/cm^3). CF: Correction factor recommended by Sprugel (1983). MSE: Mean square of error. AIC: Akaike's information criteria. Ln: Natural logarithm. The most efficient model is highlighted in bold-faced.

	Model	CF	R^2	F	P	MSE	AIC
Ln(C)	-1.46 + 0.28 DBH	1.71	0.66	165.2	<0.0001	1.07	8.26
Ln(C)	-1.46 + 0.41 H_{tot}	1.36	0.80	350.74	<0.0001	0.61	-40.0
Ln(C	1.27 - 3.6 dmf	n.s.	0.04	3.81	0.054	3.02	98.36
Ln(C)	0.52 – 0.33 ρ	n.s.	0.0006	0.05	0.82	3.16	102.14
Ln(C)	-3.26 + 2.25 Ln(DBH)	1.39	0.79	323.8	<0.0001	0.66	-34.30
Ln(C)	-1.2 + 1.54 Ln(H_{tot})	1.36	0.80	352.3	<0.0001	0.61	-40.31
Ln(C)	-1.33 – 1.14 Ln(dmf)	4.3	0.08	7.11	0.009	2.91	95.19
Ln(C)	-0.06 – 0.35 Ln(ρ)	n.s.	0.09	0.8	0.37	3.13	101.36
Ln(C)	**-1.4+1.4 Ln(DBH) + 0.94 Ln(H_{tot}) + 0.97 Ln(dmf)**	1.12	**0.92**	**486.02**	**<0.0001**	**0.34**	**-89.62**

Table 4. General allometric models to estimate above-ground carbon content (AGC; kg) based on 7 species of neotropical palms. DBH: Diameter at breast height (cm), H_{tot}: Total height (m), dmf: dry mass fraction, ρ: density of the sclerotized tissue (g/cm^3). CF: Correction factor recommended by Sprugel (1983). MSE: Mean square of error. AIC: Akaike's information criteria. Ln: Natural logarithm. The most efficient model is highlighted in bold-faced.

	Model	CF	R^2	F	P	MSE	AIC
Ln(AGC)	-1.72 + 0.28 DBH	1.7	0.66	161.41	<0.0001	1.06	7.18
Ln(AGC)	-1.72 + 0.41 H_{tot}	1.4	0.79	321.05	<0.0001	0.64	-36.27
Ln(AGC)	0.89 - 3.24 dmf	n.s.	0.04	3.14	0.08	2.96	96.62
Ln(AGC)	0.14 - 0.06 ρ	n.s.	0	0.002	0.96	3.08	99.78
Ln(AGC)	-3.48 + 2.2 Ln(DBH)	1.4	0.68	300.58	<0.0001	0.68	-31.77
Ln(AGC)	-1.45 + 1.48 Ln(H_{tot})	1.41	0.78	292.76	<0.0001	0.69	-29.98
Ln(AGC)	-1.46 - 1.04 Ln(dmf)	4.21	0.06	5.95	0.01	2.88	93.89
Ln(AGC)	-0.22 - 0.26 Ln(ρ)	n.s.	0.005	0.44	0.51	3.06	99.34
Ln(AGC)	**-1.59 + 1.46 Ln (DBH) + 0.88 Ln(H_{tot}) + 1.04 Ln(dmf)**	**1.14**	**0.91**	**284.54**	**<0.0001**	**0.28**	**-107.05**

Table 5. Coefficients of the eigenvectors of the first three first principal components calculated from the Ln-transformed values of nine morphological variables describing the morphological structure of 7 palm species from different strata in the Caribbean slope of Costa Rica.

Variable	PC1 (eigenvalue = 4) 44.40%	PC2 (eigenvalue = 1.6) 17.74%	PC3 (eigenvalue = 1.6) 15.73%
Ln root:shoot biomass	-0.04	-0.41	**0.61**
Ln root:shoot carbon	0.11	-0.13	**0.66**
Ln tissue density	-0.21	**0.56**	0.28
Ln DBH	**0.46**	-0-08	0.04
Ln H_{tot}	**0.47**	0.23	0.06
Ln dmf	-0.30	0.40	0.28
Ln total Carbon	**0.44**	0.18	0.14
Ln slenderness	0.26	**0.48**	0.05
Ln leaf area	0.38	-0.12	-0.06

Figure 1. Tissue density (A), slenderness ratio (B), dmf (C), root:shoot based on biomass (D), and root:shoot based on carbon content (E) according to palm species. Different letters next to boxplots show significant differences using Tukey HSD test.

Figure 2. Tissue density according to palm species and position along the stem in 7 species of palms in the Caribbean lowlands of Costa Rica. Species abbreviations follow Table 1. The position along the stem went from the stem apex to the base of the stem.

Figure 3. Predicted vs. observed values and residuals of the Ln of AGC in kg following the pantropical model of Chave et al. (2014), Goodman et al. (2013)´s model, and the general palm model proposed in this study (Table 3).

Figure 4. Pearson correlation matrix of morphological traits in 7 species of palms in Costa Rica. Trait abbreviations follow Table 1.

Figure 5. Ordination of species per forest strata in the space determined by the first two principal components accounting for 62.14% of the variation in 9 morphological characters defined for 7 species of tropical palms (red oval: canopy palms *Iriartea deltoidea* and *Socratea exorrhiza*, green oval: subcanopy palm *Euterpe precatoria*, and blue oval: understory palms *Asterogyne martiana*, *Prestoea decurrens*, *Chamaedorea tepejilote* and *Geonoma interrupta*).

Figure 1

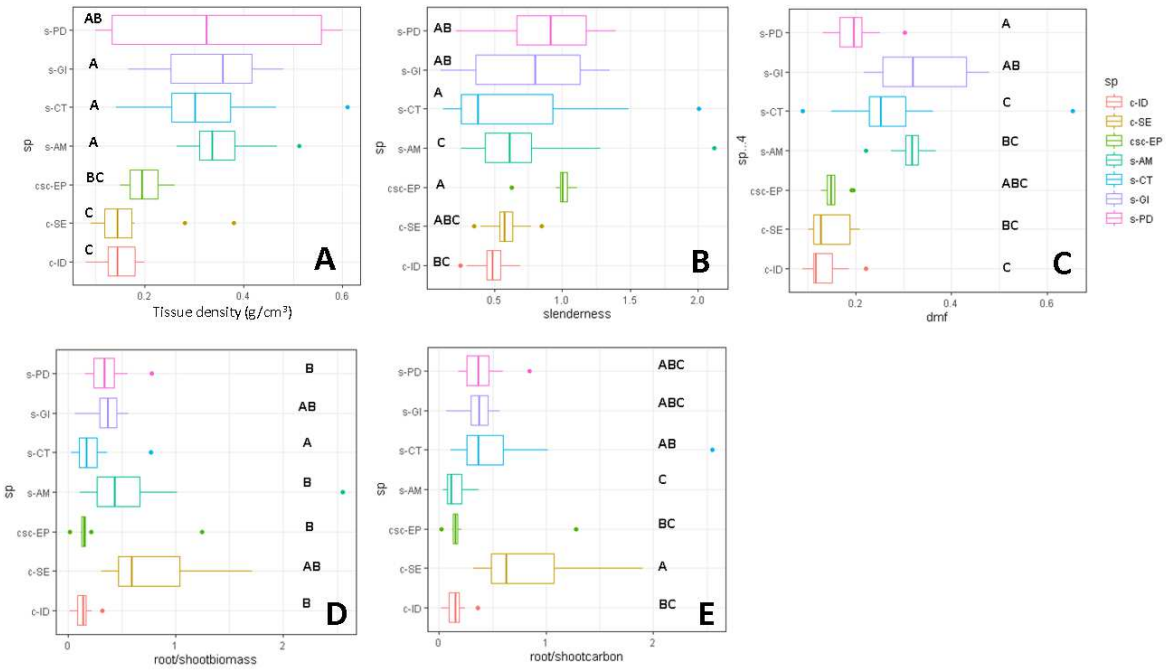
A
B
C
D
E
sp
s-PD
s-GI
s-CT
s-AM
csc-EP
c-SE
c-ID
Tissue density (g/cm³)
slenderness
dmf
root/shootbiomass
root/shootcarbon
sp..4

Figure 2

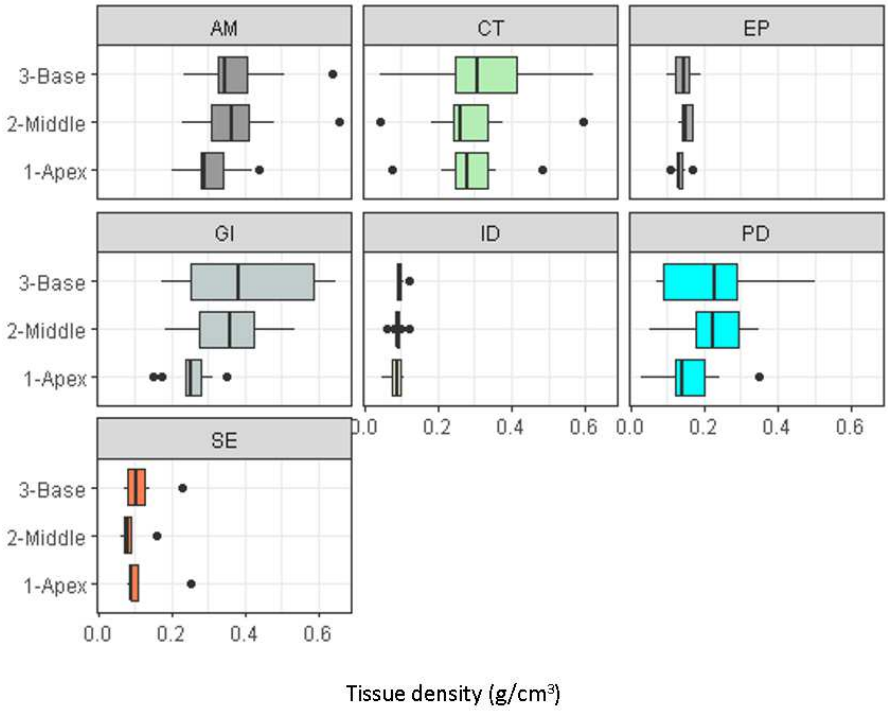
AM
CT
EP
GI
ID
PD
SE
3-Base
2-Middle
1-Apex
0.0
0.2
0.4
0.6
Tissue density (g/cm³)

Figure 3

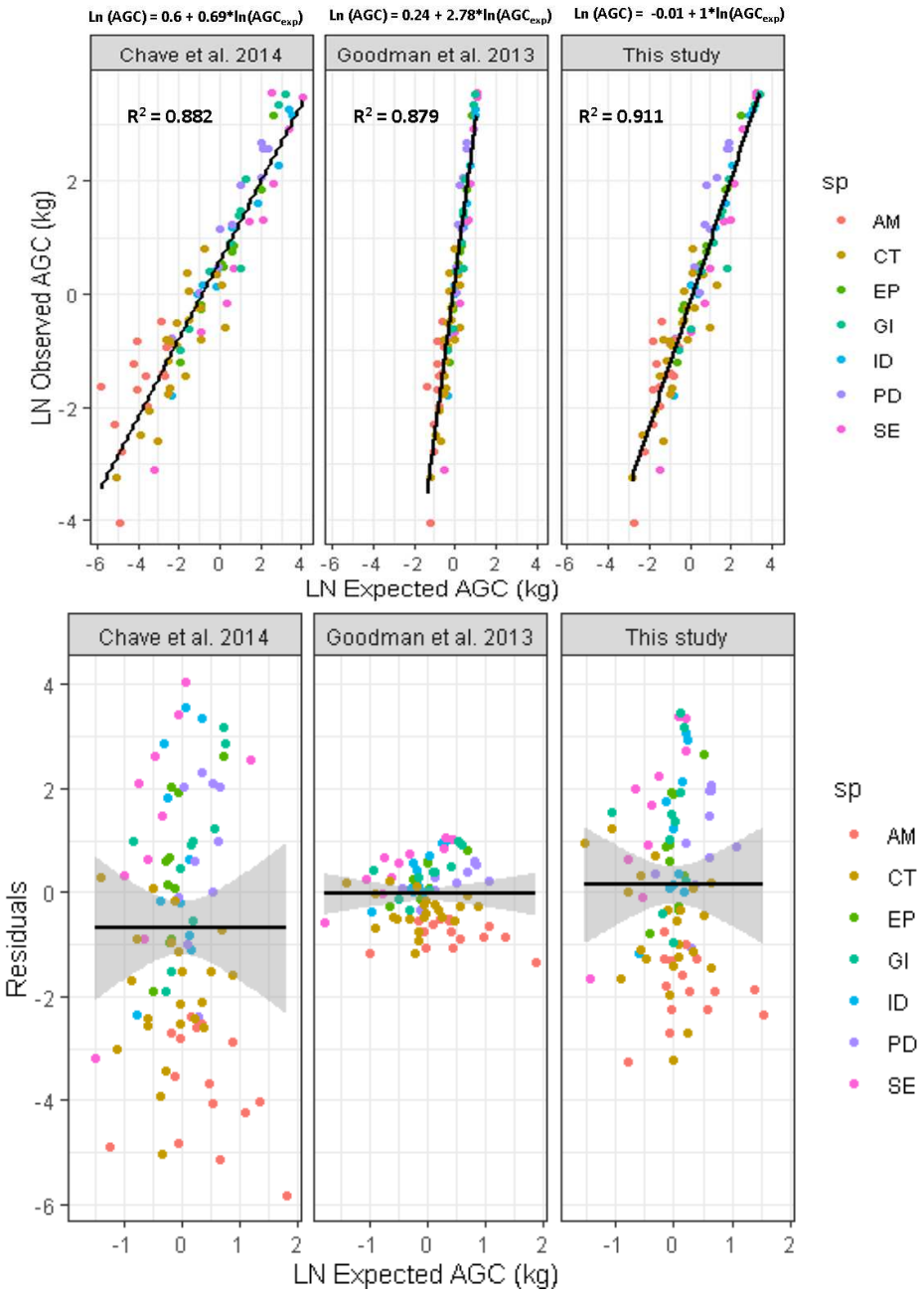
Ln (AGC) = 0.6 + 0.69*ln(AGC$_{exp}$)
Ln (AGC) = 0.24 + 2.78*ln(AGC$_{exp}$)
Ln (AGC) = -0.01 + 1*ln(AGC$_{exp}$)
Chave et al. 2014
Goodman et al. 2013
This study
R² = 0.882
R² = 0.879
R² = 0.911
LN Observed AGC (kg)
LN Expected AGC (kg)
Residuals
sp
AM
CT
EP
GI
ID
PD
SE

Figure 4

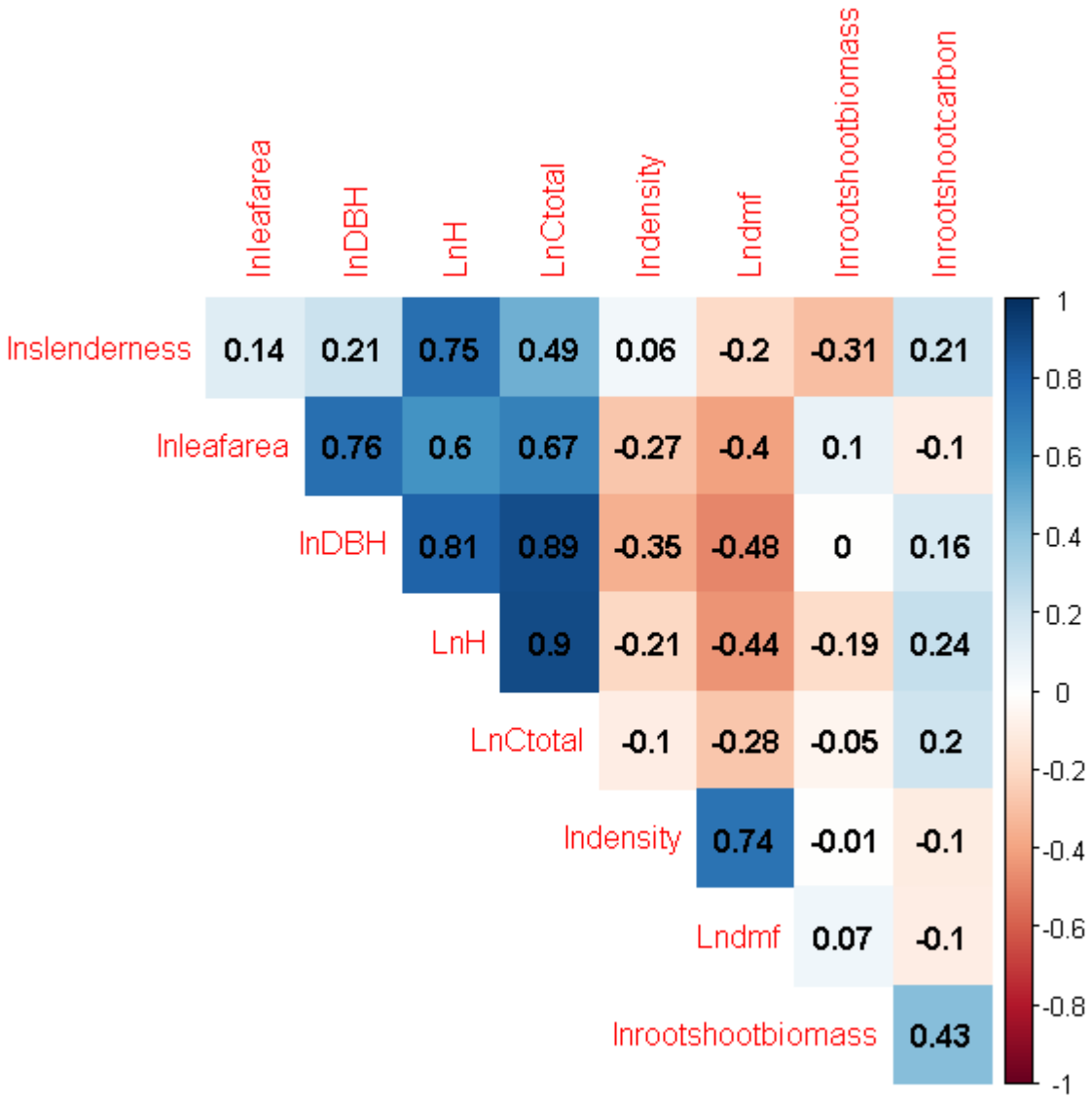
lnleafarea
lnDBH
LnH
LnCtotal
lndensity
Lndmf
lnrootshootbiomass
lnrootshootcarbon
lnslenderness
0.14
0.21
0.75
0.49
0.06
-0.2
-0.31
0.21
lnleafarea
0.76
0.6
0.67
-0.27
-0.4
0.1
-0.1
lnDBH
0.81
0.89
-0.35
-0.48
0
0.16
LnH
0.9
-0.21
-0.44
-0.19
0.24
LnCtotal
-0.1
-0.28
-0.05
0.2
lndensity
0.74
-0.01
-0.1
Lndmf
0.07
-0.1
lnrootshootbiomass
0.43
1
0.8
0.6
0.4
0.2
0
-0.2
-0.4
-0.6
-0.8
-1

Figure 5

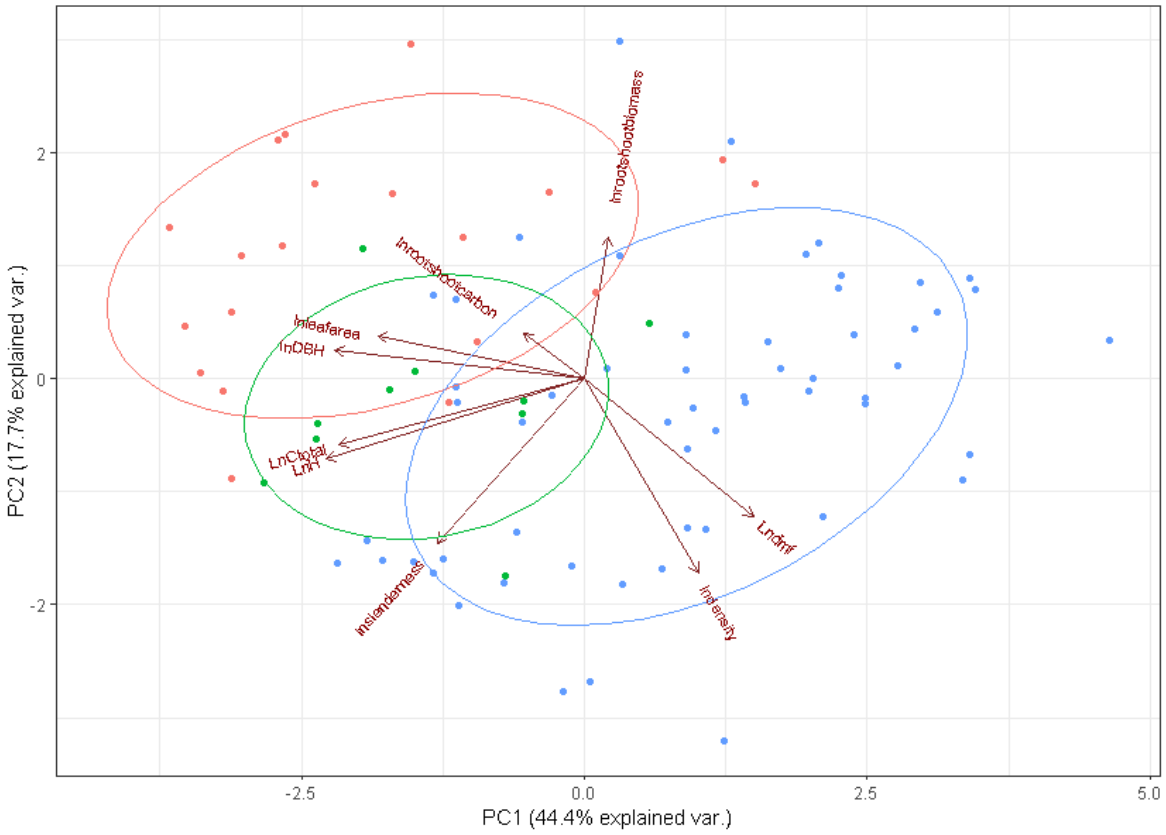
lnrootshootbiomass
lnrootshootcarbon
lnleafarea
lnDBH
LnCtotal
LnN
Lndmf
lnislandarea
lnislandarea
2
0
-2
-2.5
0.0
2.5
5.0
PC2 (17.7% explained var.)
PC1 (44.4% explained var.)